

Cite this: *RSC Advances*, 2011, 1, 1537–1541[www.rsc.org/advances](http://www.rsc.org/advances)

PAPER

# Langmuir–Schaefer films of a polyaniline–gold nanoparticle composite material for applications in organic memristive devices

Tatiana Berzina,<sup>\*ab</sup> Konstantin Gorshkov,<sup>ac</sup> Andrea Pucci,<sup>de</sup> Giacomo Ruggeri<sup>d</sup> and Victor Erokhin<sup>ab</sup>

Received 11th August 2011, Accepted 19th August 2011

DOI: 10.1039/c1ra00584g

Langmuir–Schaefer films of a polyaniline–gold nanoparticle composite were fabricated and characterized. The thickness of each deposited monolayer, determined with AFM, was found to be about 0.8 nm. The film morphology was studied by SEM, revealing the presence of embedded spherical-shaped gold nanoparticles of about 5–10 nm in diameter. The fabricated films were used as the active channel of the organic memristor. Its electric characterisation has revealed new phenomena, such as an increased working voltage range and sigmoidal voltage current characteristics that were connected to the charge trapping.

## Introduction

The concrete fabrication of memristive devices,<sup>1</sup> predicted by L. Chua,<sup>2</sup> considerably increased both experimental and theoretical research in this field,<sup>3–8</sup> because this element can be considered as the basis for new computer architectures. In particular, an electrochemically controlled polymeric heterojunction<sup>9</sup> (henceforth organic memristive device, or briefly organic memristor), for which the memristor-like properties have been extensively documented by us,<sup>10</sup> has demonstrated properties very similar to those of the biological synapses, allowing the realization of adaptive material circuits, which can be trained and show supervised<sup>11</sup> and unsupervised<sup>12</sup> learning, following the Hebbian rule.<sup>13</sup> Moreover, synthetic circuits, mimicking part of the nervous system of the pond snail *Limnea stagnalis*, responsible for learning during digestion, where organic memristive devices were used as artificial synapses, have been demonstrated.<sup>14</sup> Further progress towards bio-inspired information processing demands the presence of elements allowing the signal propagation through them only when the integrated incoming signal is higher than a certain threshold level, similar to the neuron function.

For this task, it was suggested<sup>15</sup> that gold nanoparticles (AuNPs), linked to the polyaniline (PANI) chains, by appropriate functionalization, can be used. Significant differences in the work functions of gold and PANI will provide no Schottky barrier for the electrons to enter them and a Schottky barrier for their exit. Thus, the charge will accumulate at the AuNPs until the resultant potential is higher than the barrier. It seems

important that the threshold value in such systems will be variable. Even if the height of the Schottky barrier is fixed and determined only by the difference of work functions of the materials, the potential on the AuNP will be equal to the total charge/value of the capacitance ratio, and the later is directly related to the size of the particle. Therefore, the threshold will depend on the particle diameter.

Since the working principle of the organic memristive device is based on the significant difference of the PANI conductivity in the reduced and oxidized states,<sup>16</sup> the Li<sup>+</sup> ions diffusion in the contact zone PEO–PANI is the process involved in the device performance. Therefore, complete solid state realization demands the utilization of very thin layers of PANI in the active channel in order to guarantee the best electrical properties, such as on/off conductivity ratio and optimal time of the conductivity transformation. In all our previous works such channels were realized by the PANI layer prepared by the Langmuir–Schaefer (LS) technique, as it allows for the deposition of PANI films with reproducible thickness and electrical properties.<sup>17</sup>

The aim of this work is the formation of the active channel of the memristive device from a specially synthesised composite material where AuNPs are attached to the PANI macromolecules. Close connections of the particles to the polymer chains is very important, otherwise the Schottky barriers will be too small. Finally, the organic memristive device was assembled and its electrical properties were analyzed.

## Experimental section

### Materials and method

Hydrogen tetrachloroaurate(III) trihydrate (HAuCl<sub>4</sub>, 99.9+%), 2-mercaptoethanesulfonic acid sodium salt (MESNa, ≥98.0%) and sodium borohydride (NaBH<sub>4</sub>, ≥98.0%) were purchased from Aldrich and were used without further purification. Aniline

<sup>a</sup>Department of Physics, University of Parma, Viale Usberti 7A, Parma 43124, Italy. E-mail: [tatiana.berzina@fis.unipr.it](mailto:tatiana.berzina@fis.unipr.it)

<sup>b</sup>CNR-IMEM, Parco Area delle Scienze 37/A, 43124 Parma, Italy

<sup>c</sup>Moscow Institute of Electronic Technology (Technical University), Bld. 5, Pas. 4806, Moscow 124498, Russia

<sup>d</sup>Department of Chemistry and Industrial Chemistry, University of Pisa, Via Risorgimento 35, Pisa 56126, Italy

<sup>e</sup>NEST, CNR – Istituto Nanoscienze, piazza San Silvestro 12, I-56127 Pisa, Italy

(Aldrich,  $\geq 99.5\%$ ) was purified by distillation at reduced pressure (20 mm Hg) over  $\text{CaH}_2$ .

UV-vis absorption spectra were acquired with a Perkin-Elmer Lambda 650.

Film thickness was measured *via* atomic force microscopy (AFM Solver Pro, NT-MDT). For this purpose, sharp steps were made mechanically (using a cutter) on the deposited layers and the total film thickness was determined. The AFM was operated in semi-constant mode. Measurements were carried out with a platinum-coated cantilever tip. The resonance frequency of the cantilever was about 479 kHz.

SEM images were acquired with Zeiss SUPRA 40 instrument.

236 source measure unit (Keithley) was used for the electrical measurements. The unit was linked to a PC and operated *via* MATLAB scripts, which allowed full automation of the measuring procedure.

### Preparation of the 2-mercaptoethanesulfonic acid (MESH) stabilized gold nanoparticles (Au-MESH)

2-Mercaptoethanesulfonic acid (MESH) was selected as a stabilizer for the gold nanoparticles due to the ability of the sulfonic acid moiety to efficiently protonate polyaniline, converting the polymer into the doped state.<sup>18,19</sup>

Au-MESH nanoparticles were prepared according to the literature.<sup>20</sup> In our case we used equimolar amounts of the gold precursor ( $\text{HAuCl}_4$ ) and the stabilizer (sodium 2-mercaptoethanesulfonate, MESNa), while adding a double molar amount of the reducing agent ( $\text{NaBH}_4$ ). This procedure avoids the formation of large amount of bulk Au-based precipitate during the synthesis and results in a very stable Au-MESH water solutions. After purification *via* dialysis against water, the Au nanoparticles in the protonated form, that is 2-mercaptoethanesulfonic acid stabilized gold nanoparticles (Au-MESH), were then obtained by eluting the purified Au-MESNa water solution over a proton-form cation-exchange resin. The formation of the particles was confirmed by UV-vis absorption spectroscopy. The spectrum is shown in Fig. 1.

### Preparation of the polyaniline@Au-MESH composite

The water solution containing Au-MESH nanoparticles and showing a concentration of the  $-\text{SO}_3\text{H}$  groups of  $1.21 \times 10^{-5}$  equivalents per mL, was diluted with water up to 200 mL and placed in a three-neck flask equipped with a condenser, a

dropping funnel and a mechanical stirrer. Then, 10 mL of dodecyl benzene sulphonic acid (70 wt.% solution in 2-propanol, 22.2 mmol) and 2 g (21.5 mmol) of aniline were gently added and the mixture stirred for 3 h until a white turbid dispersion is obtained. The dispersion was then cooled to  $0^\circ\text{C}$  and 5 drops of saturated  $\text{CoSO}_4$  solution (as a catalyst) was added before the dropwise addition of ammonium peroxydisulfate (APS, 5 g dissolved in 20 mL of water). The polymerization process was carried out at  $0^\circ\text{C}$  for about 5 h. The dark green dispersion was poured into an equivalent volume of methanol, and the crude precipitated composite was filtered and thoroughly washed with small portions of water and methanol until neutrality was reached. The polyaniline@Au-MESH composite was finally dried under vacuum (0.01 mm Hg) with an Au content estimated to be less than 5 wt.% by gravimetric analysis.

### Assembly of the organic memristive device

The conducting channel was formed by depositing (Langmuir-Schaefer technique) the PANI-gold nanoparticle composite material onto glass support ( $1.5 \times 0.5$  cm) with two chromium (Cr) electrodes. The spreading solution was prepared by adding chloroform to a final concentration of  $0.1 \text{ mg mL}^{-1}$ , and the solution was then carefully filtered.

Horizontal (Langmuir-Schaefer) deposition was carried out with a KSV 5000 trough. The water ( $18.2 \text{ M}\Omega$ ) purified with a Milli-Q system was used as a subphase.  $120 \mu\text{L}$  of the spreading solution was dispersed at the air-water interface and the monolayer was compressed at a rate of  $5 \text{ mm min}^{-1}$  until a surface pressure of  $10 \text{ mN m}^{-1}$  was reached. The formed monolayer was then separated in 30 independent sections by a special grid. 60 layers were deposited for all samples. The resulting film was doped in 1 M HCl for about 30 s. In approximately 20 min the doping was repeated to obtain higher and more stable values for the conductivity. Even if PANI in the composite material is in a partially conducting state, such doping was shown to improve significantly the value and stability of the conductivity.

The solid electrolyte was prepared by adding 100 mg of polyethylene oxide (PEO) to 5 mL of 0.1 M  $\text{LiClO}_4 \cdot 3\text{H}_2\text{O}$  solution. After about 24 h a homogeneous and transparent gel was formed. PEO (Mw 8 000 000) and  $\text{LiClO}_4 \cdot 3\text{H}_2\text{O}$  were purchased from Sigma. More details on the device assembly can be found in.<sup>9</sup> The scheme of the device is shown in Fig. 2.

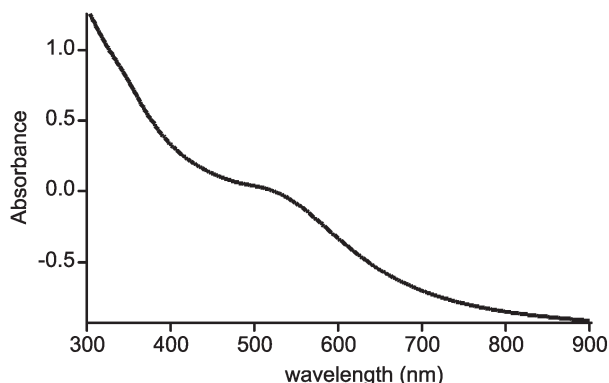


Fig. 1 UV-vis absorption spectrum of Au-MESH dissolved in water.

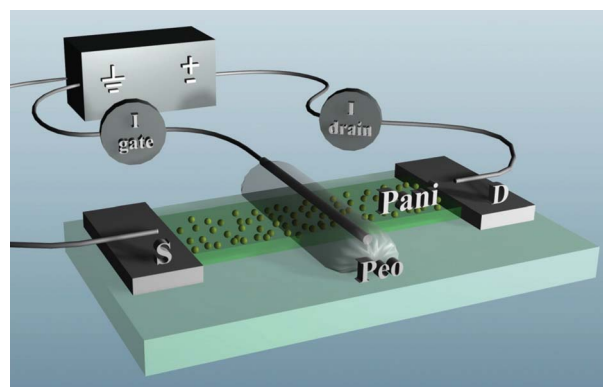


Fig. 2 Scheme of the organic memristive device.

Considering the connection of the device to the external circuit, the element shown in Fig. 2 is a two-terminal device (source and gate electrodes are connected together). The resistance of the device is a function of an ionic charge, transferred to/from the PANI channel. Therefore, the device can be considered as an organic memristor, even if it is not an ideal one. However, practically no fabricated device can be called an “ideal memristor”.<sup>21</sup> Moreover, the reported element have some features of the “memristor”, but our element has two terminals for the connection to the external circuit, as its main function during the operation was planned to mimic synapse behavior.

## Results and discussion

The first unexpected result was the partial solubility of the composite Polyaniline@Au–MESH material in chloroform. All the commercial PANI that we have used in our previous experiments was soluble in NMP (*N*-methyl-2-pyrrolidone), resulting in some difficulties in the preparation of the spreading solution. In the present case, the material was partially soluble in chloroform leaving some residue that was subsequently filtered. This phenomenon was preliminarily attributed to the lower molecular weight of the Polyaniline@Au–MESH material with respect to the commercial PANI system, which could confer to the composite a higher solubility in organic solvents. The insoluble residue could be attributed to the high molecular weight fractions of the PANI complexed by a higher local concentration of Au–MESH, which is a polyfunctional counter-anion in the composite material.<sup>22</sup>

A compression isotherm of such a compound is shown in Fig. 3.

The observed isotherm differs from that of pure PANI by the presence of a shoulder at about  $10 \text{ mN m}^{-1}$ . This shoulder is connected to the nanoparticles in the monolayer that can act as centers for the restructuring.

The morphology of the deposited films was studied by SEM and the typical image is shown in Fig. 4.

The morphology of the layer is also very similar to that of the pure PANI LB films. The film surface is not flat and the corrugation is rather high. However, for the organic memristive system such a feature is more of an advantage than a drawback, as it provides more area in contact with solid electrolyte (PEO),

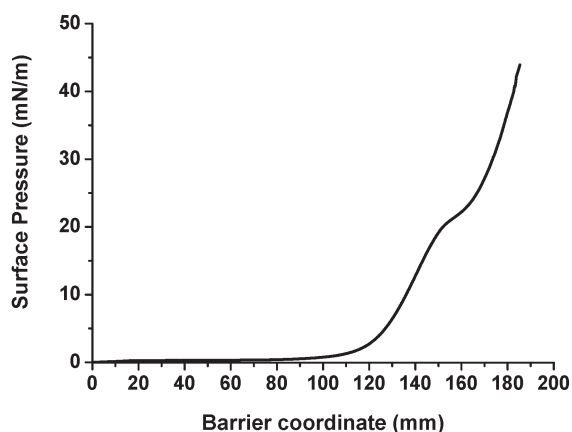


Fig. 3 Compression isotherm of the PANI–GNPs composite at the air–water interface.

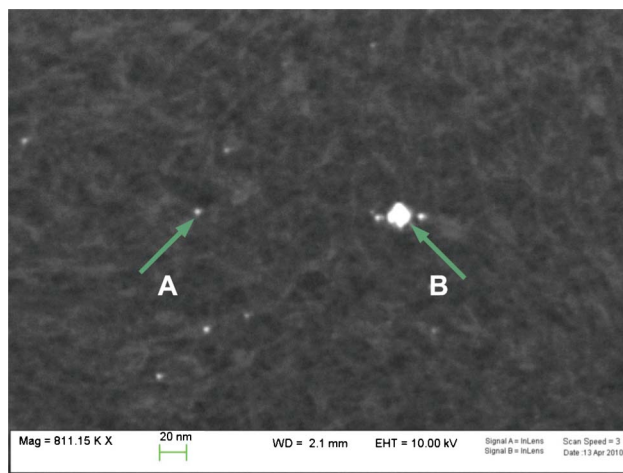


Fig. 4 SEM image of 40 layers of Polyaniline@Au–MESH deposited onto the Si support.

deposited in the central part of the conducting PANI channel. The only difference with pure PANI film is the presence of distributed AuNPs in the layer, which appeared to show a spherical shape and a diameter of about 5–10 nm (arrow A). Along with the single particles, the image also reveals the presence of aggregates which are larger in size (see Fig. 4 arrow B).

Microanalysis (Fig. 5) has confirmed that the indicated spots are gold nanoparticles.

The thickness of the transferred layers was measured by AFM on the step formed on the film. Fig. 6 reports the image of the  $10 \mu\text{m} \times 10 \mu\text{m}$  scan (a) and the height profile (b) along the line indicated in (a).

We found that the average topographic height of 24 layers was about 20 nm. Therefore, the thickness of a single molecular layer of PANI in the LS film is about 0.8 nm.

The electrical drain current characteristic of the assembled memristive device measured in the  $-1.2$  to  $+1.2$  V range (the typical working range for the organic memristor) is shown in Fig. 7. The reported characteristic demonstrates that the material used for the channel formation is adequate for providing a high conductivity ratio (about 3 orders of magnitude). However, the characteristic reveals a tendency to a saturation for voltages higher than  $+1.0$  V, which is not very typical for devices based on channels made from pure PANI material. Asymmetry of the characteristics is due to the particular features of the element structure. In fact, the reference point is connected to the S electrode, maintained at the ground potential level (Fig. 2). As the conductivity variation is due to the actual potential of the active zone (PEO–PANI contact), the polarity of the applied voltage is very important and the increase in the conductivity occurs after a certain positive voltage (higher than the oxidation potential), and the decrease in the conductivity will be at any applied negative potential).

Considering the thickness of the layer, measured with AFM, highly conducting branches of the device are characterized by about  $10 \text{ S cm}^{-1}$  conductivity, which is lower than the pure materials conductivity but rather high for a composite structure.

In order to understand this behavior the voltage range was increased. The resultant characteristic for the  $-2.0$  to  $+2.0$  V range is shown in Fig. 8.

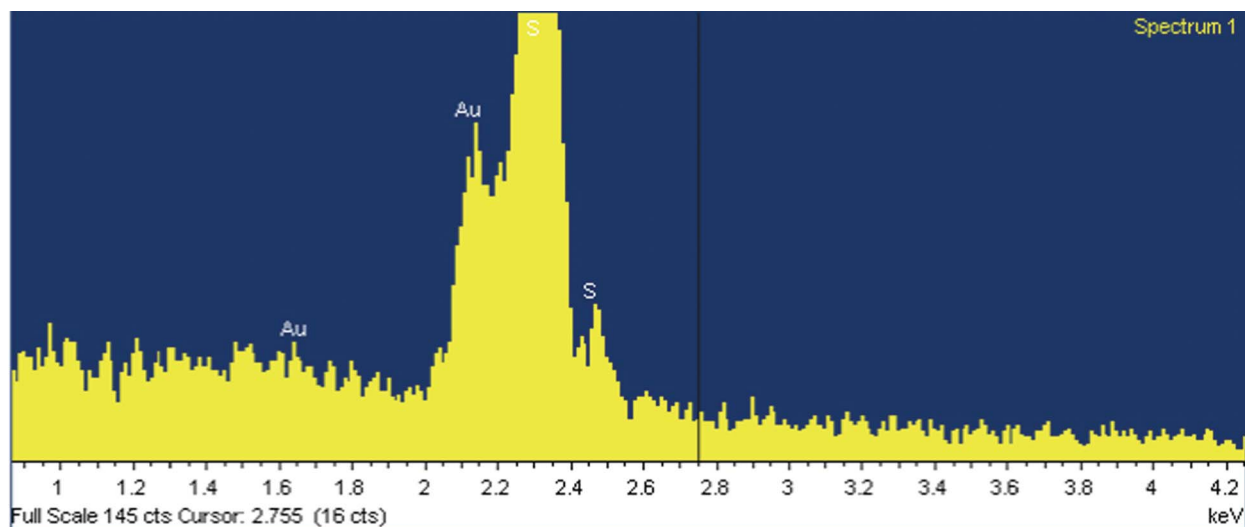


Fig. 5 EDS spectrum of the composite material

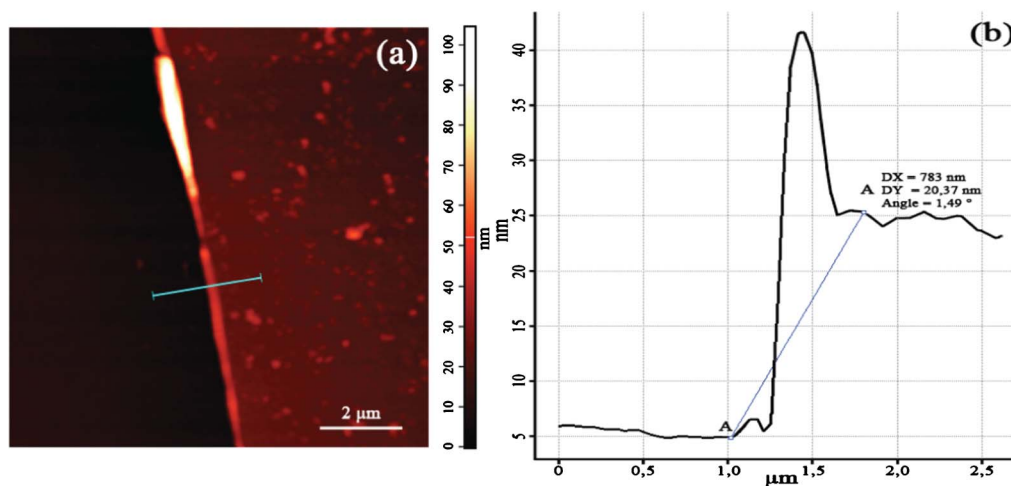


Fig. 6 AFM image of the step formed on the 24 layered Polyaniline@Au–MESH film: the 10 μm × 10 μm area (a) and the height profile (b) along the indicated line. Arrow A indicates a single particle, while arrow B indicates an aggregate.

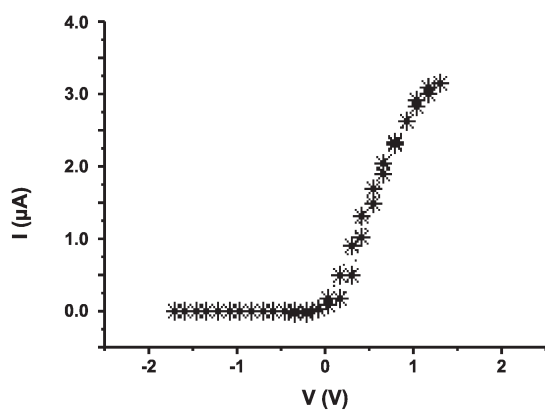


Fig. 7 Cyclic voltage current characteristics measured in the  $-1.2$  to  $+1.2$  V range.

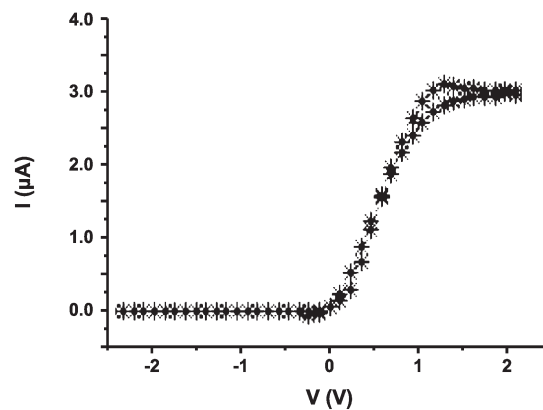


Fig. 8 Cyclic voltage current characteristics measured in the  $-2.0$  to  $+2.0$  V range.



The characteristic shows two interesting features. It has a sigmoid shape with rather small hysteresis, and is very reproducible. If the voltage range on the same sample was decreased again to  $-1.2$  to  $+1.2$  V, the measured characteristic returned to that shown in Fig. 7. This feature is very important from a practical point of view. For all our previous devices, the applied voltage was not higher than  $+1.5$  V, otherwise an irreversible decrease in the conductivity was observed due to over-oxidation of the PANI. However, the work with networks, composed of numerous memristors<sup>23</sup> demands the application of the increased voltage values, as the potential will be distributed on several devices. During the operation the memristors forming the signal pathways will have different values of resistance. Thus, we can expect that some elements will very likely be biased with more than  $+1.5$  V, which, in the case of elements without gold nanoparticles but only PANI in the channel, will result in the degradation of their electrical conductivity. In the present case, it will not occur.

The sigmoid-like characteristics can be explained qualitatively on the basis of a recently published paper<sup>24</sup> on the hybrid gold nanoparticle–organic layer field effect transistor. The paper demonstrates the hole trapping by gold nanoparticles distributed in the organic layer. The trapped charge was the reason for the memory effects observed in such systems. A similar phenomenon also occurs in our system. Hole trapping in gold nanoparticles is due to the Schottky barrier, because of a significant difference in the work-functions of Au and PANI. Trapped charges can create an electric field, opposite to the applied one, in the positive branch of the applied voltage. Thus, the higher the applied potential the more holes are trapped in the particles. Therefore, we observe the current saturation, that also prevents the PANI from over-oxidation, since the actual potential in each zone is a sum of the applied voltage and that induced by the trapped charges.

## Conclusions

In this work we have reported the deposition of LS films of AuNPs–PANI composite and their successful use as an active channel in organic memristive devices. The films were found to have a thickness of  $0.8$  nm for each transferred layer. Electrical characteristics have revealed a sigmoid-like behavior with reproducibility even after the application of higher voltages, up to  $+2.0$  V. This result is important for the design of adaptive circuits, containing a large number of statistically distributed memristors.

## Acknowledgements

We acknowledge the financial support of the Future and Emerging Technologies (FET) programme within the Seventh Framework Programme for Research of the European Commission, under the FET-OPEN grant agreement BION, number 213219. The authors are grateful to Mr. Yuri Gunaza for help in the preparation of figures.

## References

- 1 D. B. Strukov, G. S. Snider, D. R. Stewart and R. S. Williams, *Nature*, 2008, **453**, 80.
- 2 L. Chua, *IEEE Trans. Circuit Theory*, 1971, **18**, 507.
- 3 Y. V. Pershin and M. Di Ventra, *Phys. Rev. B*, 2008, **78**, 113309.
- 4 J. Wu and R. L. McCreery, *J. Electrochem. Soc.*, 2009, **156**, 29.
- 5 T. Driscoll, H. T. Kim, B. G. Chae, M. Di Ventra and D. N. Basov, *Appl. Phys. Lett.*, 2009, **95**, 043503.
- 6 S. H. Jo, K. H. Kim and W. Lu, *Nano Lett.*, 2009, **9**, 496.
- 7 K. Michelakis, T. Prodromakis and C. Toumazou, *Micro Nano Lett.*, 2010, **5**, 91.
- 8 J. Borghetti, G. S. Snider, P. J. Kuekes, J. J. Yang, D. R. Stewart and R. S. Williams, *Nature*, 2010, **464**, 873.
- 9 V. Erokhin, T. Berzina and M. P. Fontana, *J. Appl. Phys.*, 2005, **97**, 064501.
- 10 T. Berzina, S. Erokhina, P. Camorani, O. Konovalov, V. Erokhin and M. P. Fontana, *ACS Appl. Mater. Interfaces*, 2009, **1**, 2115.
- 11 V. Erokhin, T. Berzina and M. P. Fontana, *Crystallogr. Rep.*, 2007, **52**, 159.
- 12 A. Smerieri, T. Berzina, V. Erokhin and M. P. Fontana, *J. Appl. Phys.*, 2008, **104**, 114513.
- 13 D. O. Hebb, *The Organization of Behavior. A Neurophysiological Theory*. 2nd Ed. Wiley and Sons, New York, 1961.
- 14 V. Erokhin, T. Berzina, P. Camorani, A. Smerieri, D. Vavoulis, J. Feng and M. P. Fontana, *BioNanoScience*, 2011, **1**, 24–30.
- 15 V. Erokhin, in *The New Frontiers of Organic and Composite Nanotechnologies*, Erokhin, V., Ram M. K.; Yvuz, O., ed.; Elsevier, Oxford, 2007, pp. 287–353.
- 16 E. T. Kang, K. G. Neoh and K. L. Tan, *Prog. Polym. Sci.*, 1998, **23**, 277.
- 17 V. I. Troitsky, T. S. Berzina and M. P. Fontana, *Mater. Sci. Eng., C*, 2002, **22**, 239.
- 18 J. Yue, Z. H. Wang, K. R. Cromack, A. J. Epstein and A. G. MacDiarmid, *J. Am. Chem. Soc.*, 1991, **113**, 2665.
- 19 T. Berzina, A. Smerieri, M. Bernabo', A. Pucci, G. Ruggeri, V. Erokhin and M. P. Fontana, *J. Appl. Phys.*, 2009, **105**, 124515.
- 20 I. Gofberg and D. Mandler, *J. Nanopart. Res.*, 2009, **12**, 1807.
- 21 Y. V. Pershin and M. Di Ventra, *Adv. Phys.*, 2011, **60**, 145–227.
- 22 Y. Cao, P. Smith and A. J. Heeger, *Synth. Met.*, 1992, **48**, 91.
- 23 V. Erokhin, A. Schüz and M. P. Fontana, *Int. J. Unconventional Computing*, 2010, **6**, 15.
- 24 F. Alibart, S. Pleutin, D. Guerin, C. Novembre, S. Lenfant, K. Lmimouni, C. Gamrat and D. Vuillaume, *Adv. Funct. Mater.*, 2010, **20**, 330.